

# Bidirectional immobilization of affinity-tagged cytochrome c on electrodes surfaces

Florian Schröper,<sup>1,2</sup> Arnd Baumann,<sup>3</sup> Andreas Offenhäusser,<sup>1,2</sup> and Dirk Mayer\*<sup>1,2</sup>

<sup>1</sup>Institute of Bio- and Nanosystems (IBN2), Forschungszentrum Jülich, 52425 Jülich, Germany, <sup>2</sup>JARA - Fundamentals of Future Information Technology, Forschungszentrum Jülich, 52425 Jülich, Germany, and <sup>3</sup>Institute of Structural Biology and Biophysics (ISB1) Forschungszentrum Jülich, 52425 Jülich, Germany

Corresponding author: [dirk.mayer@fz-juelich.de](mailto:dirk.mayer@fz-juelich.de)

## 1. Engineering and production of genetically modified affinity-tagged cytochrome c

For novel bioelectronic and biosensorial applications the directed immobilization of redox proteins on or between nanoscopic electrodes is of major interest. Since cytochrome c (cyt c) is considered a model protein for electron transfer reactions, it was chosen for our studies. For a directed bifunctional binding of cyt c between two electrodes, two immobilization strategies were examined, i. e. electrostatic and bioaffinity binding. To allow bioaffinity binding, the cyt c sequence was genetically modified and affinity tags were introduced at desired positions. Cyt c can be immobilized to Au surfaces via internal cysteines.<sup>1-4</sup> The immobilization of horse heart cyt c by this strategy leads to a loss in redox activity<sup>4</sup>, whereas for yeast cyt c (YCC) about 5% of enzymatic activity remained in comparison to electrostatically immobilized YCC.<sup>3</sup> In contrast to horse heart cyt c, YCC contains a third cysteine residue (Cys102) close to the C-terminus. Binding of this cysteine to the Au surface may reduce the risk of protein denaturation caused by Au binding of internal cysteines (Cys14, Cys17) which in the native protein bind to the heme group.<sup>5</sup> To reduce or even completely prevent such denaturation effects and to obtain a higher yield of immobilized redox active proteins, we engineered an optimized C-terminal cys-tag to horse heart cyt c that allows directed immobilization on thioalcohol protected Au surfaces. In addition to the cys-tag, we generated a construct with a C-terminal his-tag which was used to immobilize the protein on a NiNTA functionalized SAM.<sup>6-7</sup>

In this study we used the bacterial expression system developed by Rumbley *et al.*<sup>8</sup> to produce the different horse heart cyt c variants. The expression vector pJRhrsN2 (Figure S1) carries a tandem gene coding for wildtype horse heart cyt c as well as for heme lyase from yeast which assures the correct incorporation of heme into cyt c.<sup>9</sup> Protein expression is regulated by the P(lac) promoter and for selection purposes the plasmid carries an ampicillin resistance gene (AmpR).

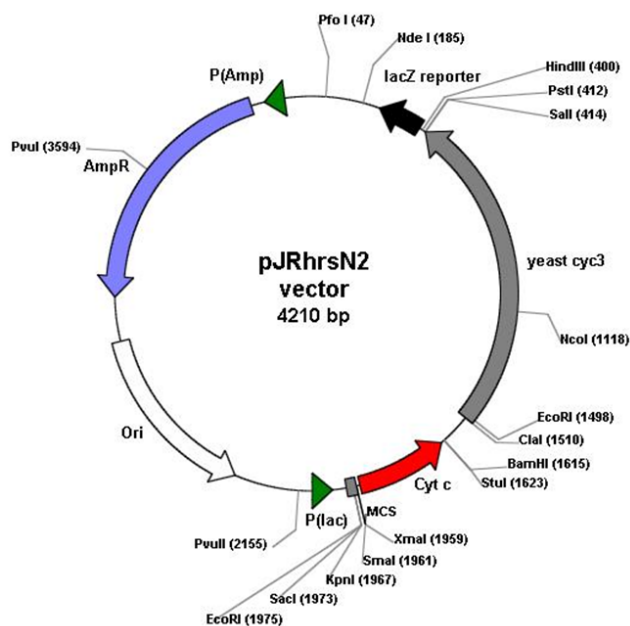


**Figure S1** Plasmid map of the recombinant *cyt c* expression vector pJRhrsN2, carrying the genes for horse heart *cyt c* and yeast heme lyase (yeast *cyc3*).

The wildtype *cyt c* gene was modified by adding *cys*- or *his*-tag encoding sequences to the 3'-end by Polymerase Chain Reaction. The amplified fragments were inserted into the expression vector via KpnI and BamHI restriction sites. Thus two expression plasmids were obtained (pJRhrsN2-Chis and pJRhrsN2-Ccys) coding for affinity-tagged *cyt c* constructs with either a C-terminal hexahistidine tag (C-*his*) or a C-terminal cysteine tag (C-*cys*) (Figure S2).

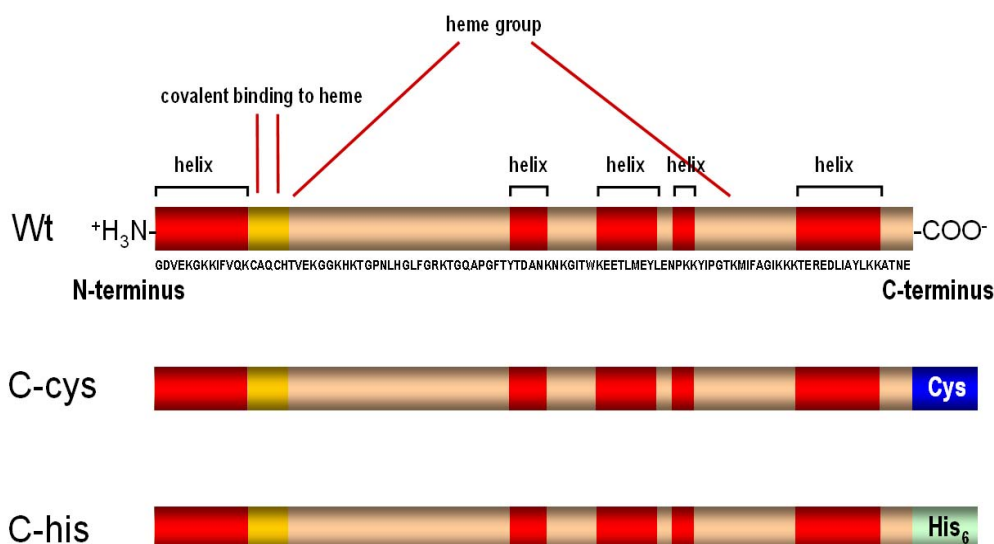


**Figure S2** Pictogram of horse heart *cyt c* (Wt). The amino acid sequence is given in the one letter code. Helical sequences (red) and junctions to the heme group are indicated. The recombinant *cyt c* with C-terminal *cys*-tag and C-terminal *his*-tag are also displayed.

The *cys*-tag was engineered to enable the functional immobilization on a Au surface covered with a thioalcohol SAM (Figure S3). For this purpose, a sequence of gold binding, hydrophobic, and hydrophilic residues were selected similar to the different functional units of the thioalcohol molecules.



**Figure S3** Amino acid sequence of the C-terminal cys-tag. It consists of two terminal cysteines, a hydrophobic alanine, two glycines and the hydrophilic amino acids serine and tyrosine.

For protein expression the constructs were transformed into *E. coli* BL21-CodonPlus-RIL (Stratagene) cells and grown in Terrific Broth at 30°C for 50h as described elsewhere.<sup>8</sup> Cells were collected by centrifugation, resuspended in lysis buffer and lysed by sonification.

Cys-tagged cyt *c* was purified by cation-exchange chromatography (CG-50, Fluka) using 20 mM sodium phosphate buffer (pH 8). The protein was eluted with 20 mM sodium phosphate buffer containing 0.5 M NaCl. His-tagged cyt *c* was purified by affinity chromatography using NiNTA agarose (Qiagen). Cells were lysed in 50 mM sodium phosphate buffer (pH 8) containing 300 mM NaCl and 10 mM Imidazol (lysis buffer). Washing was performed in lysis buffer with 20 mM Imidazol. The protein was eluted in lysis buffer containing 250 mM Imidazol. For further enrichment of cyt *c* we performed an ammonium sulfate precipitation as described.<sup>8</sup> The results of a representative purification are depicted in Figure S4. In the Coomassie-stained SDS-gel a protein of approximately 14 kDa was enriched in the elution fractions. The two protein bands of higher molecular weight present in the "Dialysate", most likely are dimeric and trimeric forms of cyt *c*.

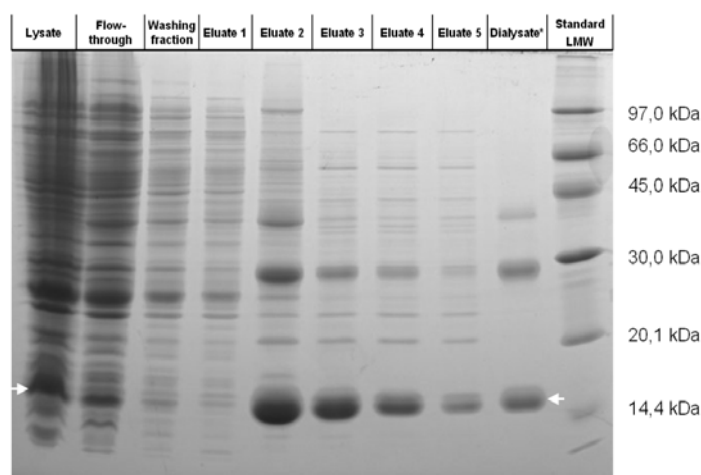


**Figure S4** Coomassie stained SDS polyacrylamide gel of samples from cyt *c* (C-cys) purification. The cyt *c* bands are labeled with arrows. For comparison a low molecular weight (LMW) standard was used. (\*) Dialysate after ammonium sulfate precipitation.

Whether the purified cyt *c* contained the heme moiety, was checked by UV/VIS spectroscopy (Lambda 900, Perkin Elmer, Waltham, MA, USA). The absorption spectra of recombinant cyt *c* were compared with those of native cyt *c* in oxidized and reduced form (Figure S5). Commercial cyt *c* in oxidized state showed the characteristic soret band at 410 nm and a broader band at 530 nm. After chemical reduction with sodium dithionite the spectra showed the slightly shifted soret band at 416 nm and two bands at 520 nm and 550 nm as described in the literature.<sup>10</sup>

Recombinant cyt *c* showed identical bands at 416 nm, 520 nm and 550 nm indicating that the protein was purified in the reduced state and displayed the absorption properties of native cyt *c*. Thus incorrect or missing heme loading can be excluded since the adsorption spectra would significantly change.<sup>11-12</sup>

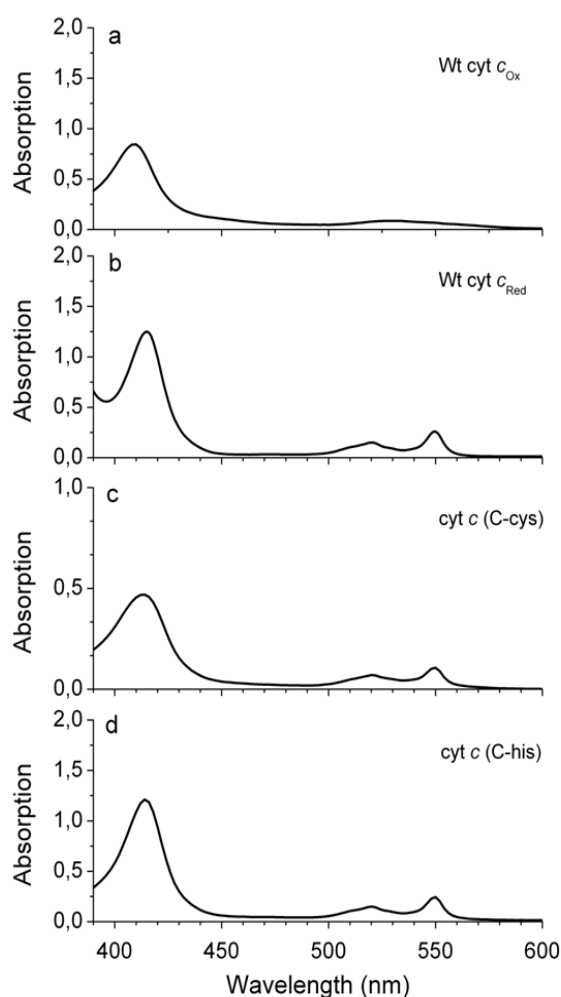


**Figure S5** UV/VIS spectra of purified recombinant cyt *c* and commercially available wildtype horse heart cyt *c* in oxidized and reduced form. Spectra were recorded from 380 nm to 600 nm.

The enzymatic integrity of recombinant cyt *c* was examined by a photochemical enzyme test.<sup>13</sup> Previously cyt *c* was fully oxidized by adding potassium hexacyanoferrate(III). The UV/VIS spectrum was recorded and showed the expected absorption bands. Addition of the enzyme cyt *c* reductase (0.005 – 0.025 U; porcine heart; Sigma-Aldrich) and NADH (1 mM; Sigma-Aldrich) lead to a change in the absorption spectrum within five minutes due to the formation of the reduced form of cyt *c* (Figure S6). These results show that cyt *c* reductase efficiently binds to recombinant cyt *c* (cys-tagged and his-tagged) and reduces it.

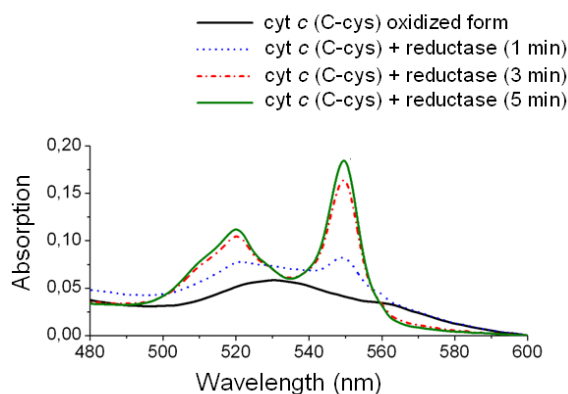


**Figure S6** UV/VIS spectra of recombinant cyt *c* (C-cys) before (black curve) and 1 min, 3 min and 5 min after the addition of cyt *c* reductase and NADH.

## 2. Immobilization studies

Immobilization efficiency of commercial and recombinant cyt *c* was investigated by Kretschmann Type Surface Plasmon Resonance Spectroscopy using a Biosuplar 3 Reflectometer (Analytical  $\mu$ -Systems/ Mivitec GmbH, Sinzig, Germany). Au covered glass slides (Analytical  $\mu$ -Systems/ Mivitec GmbH, Sinzig, Germany) were functionalized with carboxylic groups for electrostatic immobilization using MUA as SAM and a thioalcohol as SAM for binding of the cys-tag. Incubation times were at least 2 h in 10 mM ethanolic solution. For his-tag immobilization Au glass slides were functionalized by NINTA as described elsewhere.<sup>6-7</sup> After rinsing with ethanol and MilliQ water, protein adsorption was initiated in a flowthrough-cell. A 10  $\mu$ M protein solution in 5.78 mM sodium phosphate buffer (pH 7) was flushed over the surface (0.26 ml/min). After protein binding saturated, the surface was rinsed with buffer for several minutes. To achieve bifunctional immobilization of the protein we injected a solution of Au nanoparticles functionalized with carboxylic groups (5 nm gold colloid suspension, Sigma-Aldrich; 1:1 diluted in sodium phosphate buffer) and monitored the electrostatic binding of the particles to the affinity tag-immobilized cyt *c*. Irreversible binding events were monitored for cys- and his-tagged cyt *c* whereas no significant binding was observed for electrostatically immobilized native cyt *c*. In addition to the SPR measurements, electrostatic nanoparticle binding on top of his-tagged cyt *c* was investigated by AFM measurements (Figure S7). AFM measurements were performed in tapping mode at room temperature with a MultiMode AFM/STM (Veeco/Digital Instruments, Santa Barbara, CA) equipped with a Nanoscope IV controller and a 15- $\mu$ m scanner. Commercially available silicon cantilevers have been employed with resonance frequencies between 260 and 300 kHz. Figure S7a shows a Au(111) surface homogeneously covered with his-tag immobilized cyt *c*. Figure S7b shows the same sample after 15 min incubation with Au nanoparticle solution and subsequent rinsing with buffer. The surface was densely covered with Au nanoparticles (surface coverage  $\sim$ 80-90%). The recombinant cyt *c* was bifunctionally immobilized between the Au surface and the nanoparticles as illustrated in Figure S7c.

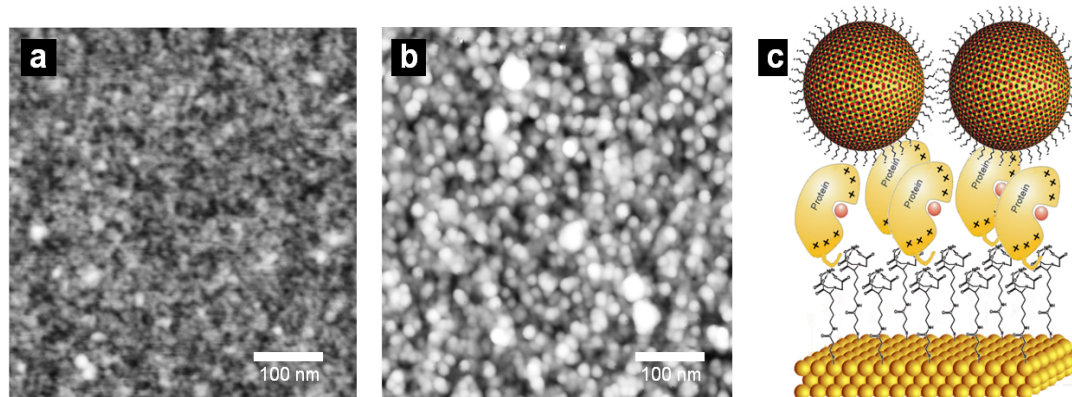


**Figure S7** Electrostatic binding of Au nanoparticles: (a) Contact mode AFM image of a Au(111) surface covered with his-tag immobilized cyt *c*. (b) Same surface after incubation in Au nanoparticle solution and subsequent rinsing with buffer. (c) Schematic view of the Au nanoparticle immobilization.

### 3. Cyclic voltammetry

The redox activity of immobilized recombinant cyt *c* and native cyt *c* was investigated by cyclic voltammetry with an EG&G 283 potentiostat (Princeton Applied Research, Princeton, NJ, USA). Proteins were immobilized either by electrostatic immobilization or by the affinity tag on SAM covered Au(111) electrodes. Electrodes were prepared by flame annealing and incubation in ethanolic SAM solution as described above. For protein immobilization the electrodes were incubated in 10  $\mu\text{M}$  cyt *c* solution in 5.78 mM sodium phosphate buffer (pH 7) for at least 5 min (electrostatic binding) and 60 min (tag immobilization), respectively. Before starting the electrochemical recording the cyt *c* covered electrodes were rinsed with buffer thoroughly to remove unbound protein. A considerable redox signal was observed for C-cys immobilized via its tag on a Au electrode covered with MPhOH (Fig. 2b). The determined mean charge density ( $\sigma_m$ ) was higher than for electrostatically bound proteins, which accounts for an effective immobilization process and a good electronic coupling between electrode and protein. Electron transfer was also observed when C-cys was immobilized on other thioalcohol SAMs although the redox signals were less pronounced. Thus immobilization of the protein by its cys tag on short aliphatic thioalcohols, seems not to result in a such favourable orientation for efficient electron transfer.

**Table 1.** Electrochemical data for cysteine-immobilized cyt *c* on Au(111) covered with different SAMs determined from cyclic voltammograms recorded with 100 mV/s.

	$E_p$ [mV]	$\sigma_m$ [ $\mu\text{C}/\text{cm}^2$ ]	$B_n$ [%]
Cyt <i>c</i> (C-cys) / MEOH	80	0.5	30
Cyt <i>c</i> (C-cys) / MPOH	97	0.2	9
Cyt <i>c</i> (C-cys) / MPhOH	69	1.3	75

Figure S8a shows the cyclic voltammogram of electrostatically immobilized his-tagged cyt *c* on Mercaptopropionic acid (MPA). The his-tagged cyt *c* exhibits a defined and reproducible redox signal, although the separation of the oxidation and reduction peak ( $\sim 100$  mV) indicates a kinetic limitation as it is usually seen for long chain molecules.<sup>14-17</sup> From this result it can be assumed that the his-tagged cyt *c* obtained unfavorable orientation that results in an increased distance between electrode and redox centre, but still allows an efficient electron transfer. In contrast, the cys-tagged cyt *c* did not show such a peak separation. A reason for the different orientations might be

the positively charged hexahistidine tag, which may cause a changed charge distribution on the protein surface favoring a different orientation upon electrostatic binding.

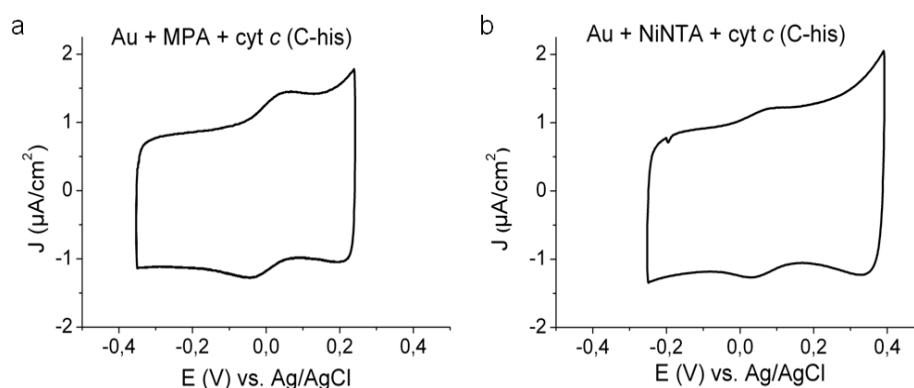


**Figure S8** Cyclic voltammograms of (a) electrostatically immobilized his-tagged cyt *c* on MPA and (b) cyt *c* immobilized by the his-tag on NiNTA functionalized Au(111) electrode in 5,78 mM sodium phosphate buffer (pH 7) at a scan rate of 100 mV/s.

The cyclic voltammogram of cyt *c* immobilized by its C-terminal his-tag on a TSP+NiNTA covered electrode shows a stable and pronounced redox peak with no significant separation (Figure S8b). This confirms the efficient electron transfer between electrode and his-tagged cyt *c*. Taken together, we can conclude that a reversible electron transfer between electrode and cyt *c* is possible when the protein is immobilized either electrostatically or by its C-terminal affinity tags (cys- and his-tag).

To determine whether electron transfer is also possible through the bifunctionally immobilized cyt *c*, we used an electroenzymatic reaction. Cyt *c* reductase binds to the lysine-rich region of oxidized cyt *c*<sup>18-19</sup> and catalyses its reduction by transferring electrons from NADH to the heme group. Cyt *c* oxidase binds to the same region, but catalyzes the oxidation of cyt *c* by transferring electrons from the heme group to oxygen.<sup>18-19</sup> We immobilized cyt *c* via the affinity tags (his-tag or cys-tag) to a Au(111) electrode surface as described above and recorded the cyclic voltammogram (scan rate 2 and 5 mV/s). After the addition of 0.8 mg/ml reductase (porcine heart, Sigma-Aldrich) and 7.5 mM NADH (Sigma-Aldrich) we observed an increase of the anodic current due to the electron transfer from NADH via cyt *c* reductase to the heme group of cys-tagged as well as the his-tagged (Fig. S9) cyt *c*. This increase indicates an iterative electroenzymatical reaction during the anodic potential scan, where the immobilized protein is oxidized electrochemically followed by an instantaneous enzyme driven reduction.

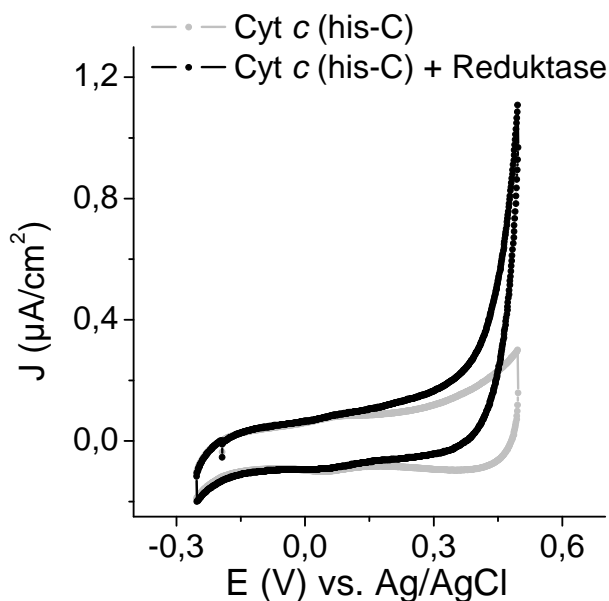


**Figure S9** Cyclic voltammograms of his-tag immobilized cyt *c* (grey curve) and electroenzymatic reaction catalyzed by cyt *c* reductase (black curve) recorded with a scan rate of 5 mV/s.

Additionally, we used the enzyme cytochrome *c* oxidase together with cys-tag immobilized cyt *c* to monitor the inverse electroenzymatic reaction. Cytochrome *c* oxidase binds to the same lysine rich region of cyt *c* as cyt *c* reductase. In this configuration, electrons are transferred from the electrode to cyt *c*, then towards the oxidase and finally to oxygen. Adding cytochrome *c* oxidase (purified from horse heart according to Yoshikawa *et al.*)<sup>20</sup> instead of reductase to the immobilized cyt *c*, induced the inverse reaction and led to a strong increase of the cathodic current. In the case of electrostatically immobilized cyt *c*, we were not able to detect any kind of electroenzymatic reaction. This is probably due to the fact that the lysine-rich region, which is faced down to the electrode side, is not accessible for reductase or oxidase binding.

#### References:

1. A. G. Hansen, A. Boisen, J. U. Nielsen, H. Wackerbarth, I. Chorkendorff, J. E. T. Andersen, J. Zhang, J. Ulstrup, *Langmuir* **2003**, *19*, 3419.
2. B. Bonanni, D. Alliata, A. R. Bizzarri, S. Cannistraro, *ChemPhysChem* **2003**, *4*, 1183.
3. H. A. Heering, F. G. M. Wiertz, C. Dekker, S. de Vries, *J. Am. Chem. Soc.* **2004**, *126*, 11103.
4. H. Yue, D. H. Waldeck, *Current Opinion in Solid State and Materials Science* **2005**, *9*, 28.
5. T. Ruzgas, A. Gaigalas, L. Gorton, *J. Electroanal. Chem.* **1999**, *469*, 123.
6. a) K. Ataka, F. Giess, W. Knoll, R. Naumann, S. Haber-Pohlmeier, B. Richter, J. Heberle, *J. Am. Chem. Soc.* **2004**, *126*, 16199; b) M. Conti, G. Falini, B. Samorì, *Angew. Chem. Int. Ed.* **2000**, *39*, 215–218.
7. D. Mayer, K. Ataka, J. Heberle, A. Offenhäusser, *Langmuir* **2005**, *21*, 8580.
8. J. N. Rumbley, L. Hoang, S. W. Englander, *Biochemistry* **2002**, *41*, 13894.
9. W. B. Pollock, F. I. Rosell, M. B. Twitchett, M. E. Dumont, A. G. Mauk, *Biochemistry* **1998**, *37*, 6124.

10. E. Margoliash, O. F. Walasek, *Methods in Enzymology* **1967**, *10*, 339.
11. E. Santoni, S. Scatraglia, F. Sinibaldib, L. Fioruccib, R. Santuccib, G. Smulevich, *Journal of Inorganic Biochemistry* **2004**, *98*, 1067.
12. E. Chen, C. J. Abel, R. A. Goldbeck, D. S. Kliger, *Biochemistry* **2007**, *46*, 12463.
13. H. R. Mahler, *Methods in Enzymology* **1955**, *2*, 688.
14. S. Song, R. A. Clark, E. F. Bowden, M. J. Tarlov, *J. Phys. Chem.* **1993**, *97*, 6564.
15. Z. Q. Feng, S. Imabayashi, T. Kakiuchi, K. Niki, *J. Chem. Soc., Faraday Trans.* **1997**, *93*, 1367.
16. A. Avila, B. W. Gregory, K. Niki, T. M. Cotton, *J. Phys. Chem. B* **2000**, *104*, 2759.
17. K. Niki, J. R. Sprinkle, E. Margoliash, *Bioelectrochemistry* **2002**, *55*, 37.
18. R. E. Dickerson, R. Timkovich, *Enzymes, 3rd Ed.* **1975**, *11*, 397.
19. L. Smith, H. C. Davies, M. E. Nava, *Biochemistry* **1976**, *15*, 5827.
20. S. Yoshikawa, M. G. Choc, M. C. O'Toole, W. S. Caughey, *J. Biol. Chem.* **1977**, *252*, 5498.